Phylogenomic analysis of the Lake Kronotskoe species flock of Dolly Varden charr reveals genetic signatures of sympatric radiation

Katherine C. Woronowicz[1], Evgeny V. Esin[2], Grigorii N. Markevich[3], Jacob M. Daane[4], Matthew P. Harris[1]*, Fedor N. Shkil[2,5]*

Author affiliations

1 Department of Orthopaedics, Boston Children's Hospital and Department of Genetics, Harvard Medical School, Boston, MA 02115

2. AN Severtsov Institute of Ecology and Evolution, RAS; Leninskiy-33, 119071 Moscow, Russian Federation

3. Kronotsky Nature Biosphere Reserve; Ryabikova-48, 68400 Yelizovo, Russian Federation

4. Department of Biology and Biochemistry, University of Houston, Houston, TX 77204

5. NK Koltzov Institute of Developmental Biology, RAS; Vavilova-26, 119334 Moscow, Russian Federation

Significance Statement

A radiation of Dolly Varden Charr (*Salvelinus malma*) in Lake Kronotskoe provides a case study of the genetics of adaptation and morphological evolution.

Abstract

Recent adaptive radiations provide evolutionary case studies which can be parsed to reveal the relationship between genomic variation and the origins of distinct phenotypes. Sympatric radiations of the charr complex (genus *Salvelinus*) present a trove for comparative genomics as charrs have repeatedly diversified into multiple morphs with distinct feeding specializations. However, stereotypical species flocks are assemblages of only two to three lineages. However, a species flock of Dolly Varden charr (*Salvelinus malma*) in Lake Kronotskoe contains at least seven lineages, each with defining morphological and ecological traits. This is the most extensive radiation described for the genus. Here, we perform the first genome-wide analysis of this species flock to parse the genetic foundations of adaptive change. Our data support distinct, reproductively isolated lineages with little hybridization. We also find that specific selection on thyroid and craniofacial genes forms a shared basis for the radiation. The data also implicate thyroid signaling in subsequent lineage specification. These results delineate a clear genetic basis for the diversification of specialized lineages, and highlight the role of developmental mechanisms in shaping the forms generated during adaptive radiation.

Introduction

The Salmonoid fishes of the genus *Salvelinus* represent an exceptional example of parallel evolution and trophic adaptation to new environments (Klemetsen, 2010). Charr are remarkably variable with naturally occurring, and morphologically distinct populations implementing varied life histories, including complete and partial anadromy, as well as freshwater riverine and lacustrine residency (Lecaudey et al., 2018; Osinov et al., 2021; Taylor, 2016). Interestingly, freshwater resident populations frequently establish species flocks of stereotypical morphologies, each associated with an ecological niche (Esin et al., 2020; Jacobs et al., 2020; Maitland et al., 2007; Markevich et al., 2018; Nordeng, 1983; Sandlund et al., 1992; Simonsen et al., 2017; Walker et al., 1988). Within a sympatric population, varying diets, depth preferences, and disparate spawning intervals are commonly observed (Jonsson & Jonsson, 2001; Klemetsen, 2010). Within independent lacustrine *Salvelinus* radiations, specific morphological adaptations have repeatedly evolved (Klemetsen, 2010). *Salvelinus* charrs have repeatedly radiated into multiple sympatric morphs with distinct feeding specializations analogous to those seen in the evolution and diversification of both African and South American cichlids (Barluenga et al., 2006; Malinsky et al., 2015; Malinsky et al., 2018) and African and Asian barbs (Levin et al., 2020; Myers, 1960; Nagelkerke & Sibbing, 2000). The

variability within, and between, charr radiations proffers important genetic case studies to uncover mechanisms of rapid morphological diversification. Such parallel events suggests that these populations experience similar selective pressures, or, alternatively that there are genetic biases shaping the morphologies that arise. The genetic mechanisms that enable charr to generate such distinct morphologies, however, are not well defined. It has been argued that shifts in developmental timing may underlie these common transitions to specialized morphologies among charrs (Esin et al., 2018). In this model, development shapes radiations by imparting a common axis of change. By just a few genetic modifications, early and pleiotropic developmental shifts may permit charr their exceptional capacity for adaptive radiations.

The Lake Kronotskoe radiation of Dolly Varden (*Salvelinus malma*) is unique amongst charrs, as it contains at least seven reproductively isolated phenotypes associating with different ecological niches (Markevich et al., 2018). This radiation is currently the broadest observed within resident lacustrine populations of this genus and, indeed, among salmonids more broadly (Markevich et al., 2018). Recent work has characterized genome-wide changes in species flocks of Alpine whitefishes (Coregonus spp.), however, those flocks comprise of up to six species with varying morphologies (De-Kayne et al., 2022a). Lake Kronotskoe is one of several volcanogenic lakes of the Kamchatka peninsula (**Figure 1A**) originating approximately 12,000 years ago due to a lava flow damming the ancestral river (**Figure 1B)** (Braitseva et al., 1995). The resulting landlocked Dolly Varden population diversified within the new lacustrine environment, leading to prominent changes in craniofacial form and new feeding strategies (**Figure 1C, D**) (Esin et al., 2020; Markevich et al., 2018). A major axis of change is proportional jaw length, seen in piscivorous Longhead and deep-water benthivorous Bigmouth morphs, as well as the modulation of frontonasal proportions found in the Nosed morphs. The deep-water omnivorous Smallmouth morph has an increase in eye size in relative proportion to the cranium (**Figure 1C, D**). Enlarged eye size is widespread among deep-dwelling resident charr lineages in other lakes and may suggest specialization for foraging in low light conditions (Klemetsen, 2010). The varied Lake Kronotskoe charrs show strict natal homing with some morphs spawning in tributaries and other morphs spawning within the lake (Markevich et al., 2021). The morphs also exhibit differential annual windows for the timing of reproduction, which reinforces reproductive isolation and facilitates sympatric radiation (Evgeny V. Esin, Grigorii N. Markevich, Nikolai O. Melnik, et al., 2021).

Here, we survey phylogenomics of the Dolly Varden radiation within Lake Kronotskoe to frame the genetic context of their diversification as well as the foundation for the morphological and physiological adaptations of these specialized lineages.

Genome wide assessment of variability within and between Lake Kronotskoe Dolly Varden morphs

To investigate variation across the charr genome, we performed genome-wide targeted capture, of coding and non-coding loci of Dolly Varden charr from Lake Kronotskoe using a custom, pan-Salmonidae capture array. Targeted capture allows cross-clade sequence comparisons in order to identify lineage-defining variation. Additionally, because we pooled multiple individuals per sample, this approach also facilitates analysis of variation and fixation within each lineage. Similar approach have been recently used to assess variation in

Belonifomes (Daane et al., 2021), rockfishes (Treaster et al., 2022), and notothenioids (Daane et al., 2019) allowing for clade-wide analysis of genomic variation and phylogenetic parsing of selective signals.

We constructed a pan-Salmonidae capture-array consisting of 558,882 bait sequences designed against conserved Atlantic Salmon (*Salmo salar*) and Rainbow Trout (*Oncorhynchus mykiss*) genomic sequences, targeting 97Mb of total sequence **(Figure 2 – figure supplement 1**). Coding regions constitute 83.8% of targeted regions with conserved non-coding, ultraconserved non-coding, and miRNA hairpins comprising the remaining 16.2% of targeted regions. With our capture methodology and analysis pipeline, bait sequences successfully hybridize with targeted elements harboring up to 15% deviation in sequence identity (Mason et al., 2011), thereby allowing recovery and subsequent analysis of sequence variability. Pairwise analyses between homologous loci are then used to distinguish fixed and variable loci between morphs. Genes associating with variation were identified by making strategic comparisons within a phylogeny focused on character diversification (Daane et al., 2015). For outgroup analysis, we sampled anadromous Dolly Varden charr from the local Kamchatka river basin, which is adjacent to, but isolated from, that of Lake Kronotskoe (**Figure 1B**). We also sequenced a single *S. leucomaenis* individual which was collected from the same catchment as the Dolly Varden charr.

For each group, we recovered approximately 90% of the targeted elements sequenced to a mean depth of 25-52 reads (**Figure 2 – Supplementary Table 1**). We detected substantial variation within each lineage as well as the putative ancestral population (avg π in Dolly Varden = 0.003) supporting pairwise analysis to detect and compare shared and unique variation within each lineage. Loci underrepresented in our capture were limited and represented as general gene classes. These elements recovered with low coverage are similar to those observed in other broad capture approaches (**Supplementary Table 2**)(Daane et al., 2021; Daane et al., 2019; Treaster et al., 2022).

Genetic differentiation and relationships among Dolly Varden morphs

As a first analysis, we conducted Principal Components Analysis (PCA) to visualize the relationships among our lacustrine and anadromous Dolly Varden samples and outgroup *S. leucomaenis*. PC1 separates *S. leucomaenis* from Dolly Varden and from the members of the Dolly Varden species flock (**Fig. 2A**), while PC2 broadly groups lineages according to ecological niche. Notably, all three Nosed morphs cluster quite tightly.

Prior hypotheses of causes of this radiation argued for multiple-step diversification based on changes in resource utilization and accompanying feeding specializations leading to the extant morphs (5). We investigated relationships among Lake Kronotskoe charrs through reconstruction of the phylogeny given our substantial sequence data. We used IQ-TREE to derive a phylogeny from a dataset containing 622,831 variant sites, of which 22,701 variants were informative (Nguyen et al., 2015). Our data support the existence of the described distinct morphs, with each node having high bootstrap support (**Figure 2B**). Our analysis clusters Longhead and White morphs within a lineage that is an outgroup to the clade consisting of the Bigmouth, Smallmouth, and Nosed morphs. Nosed lineages differentiate as a distinct clade with Nosed 2 as an outgroup to Nosed lineages 1 and 3. As the Nosed 2 population associates so closely with Nosed 3 via PCA (**Figure 2A**), we focused subsequent analyses on disentangling the differentiation between Nosed morphs 1 and 3.

The anadromous and resident lacustrine Dolly Varden morphs are clearly genetically differentiated within ecologically specialized lineages, having pairwise mean Fst consistent with distinct populations (**Figure 2C**) (**Supplementary File 1**). The greatest pairwise differentiation is found between the anadromous Dolly Varden charr and lacustrine deep-water Bigmouth morph (Fst = 0.127). Notably, each lacustrine lineage is more differentiated from the anadromous Dolly Varden population than from any other lacustrine lineage. Furthermore, lacustrine lineages are similarly differentiated from the putative ancestral riverine Dolly Varden population. Within the species-flock, the least differentiated pairing is between the lacustrine Nosed 1 and Nosed 3 morphs (Fst = 0.047) consistent with their phylogenetic relationship. Although informative of broad patterns of divergence, these values are likely underestimations of genetic differentiation due to the conserved element-based dataset biasing analysis to regions having an inherent constraint on variation.

An analysis of introgression within the clade further supports the existence of distinct lineages, albeit with the presence of some incomplete lineage sorting. Significant introgression was identified in 80% of the 20 possible trios (DSuite; Holm-Bonferoni FWER < 0.01) in patterns which deviated from the topology of the phylogeny (**Supplementary Table 3**) (Malinsky et al., 2021). Despite observed significance, the introgression values are relatively small when compared to the recent timeline of the Lake Kronotskoe radiation. The Bigmouth and Nosed 1 morphs were ascribed the greatest excess of allele sharing (D_{tree} = 4.2%) (**Supplementary Table 3**). We further calculated f_4-admixture ratios and used f-branch statistics to disentangle the interrelatedness of admixture signals among morphs that share common internal phylogenetic branches (**Figure 2D**). The greatest proportions of shared alleles are between the Bigmouth morph and the Nosed 1 morph (f-branch = 9.0%), between the Bigmouth morph and the Nosed 3 morph (f-branch = 8.3%), and between the White morph and the ancestor of the Nosed 1 and Nosed 3 morphs (f-branch = 5.9%). The f-branch statistic further supports that the Lake Kronotskoe lineages differentiated while maintaining relative genetic isolation.

To determine the extent to which Nosed 1 and Nosed 3 share common introgressed loci with Bigmouth, we calculated D in sliding windows (40 variant windows, 20 variants step-size) for Smallmouth, Bigmouth, Nosed 1 (mean = 0.046, SD = 0.22) and Smallmouth, Bigmouth, Nosed 3 (mean = 0.041, SD = 0.21). Anadromous Dolly Varden served as the outgroup for all analyses of introgression. Among sliding windows with D >= 0.8 (32 of 10,617 windows for S, B, N1; 28 of 10,790 windows for S, B, N3), we observed shared, isolated regions of the genome with signatures of admixture (**Supplementary File 2**). Among these, we detected a large interval with evidence for shared introgression between Bigmouth and Nosed morphs 1 and 3 (mean D for the interval = 0.53 for S, B, N1; 0.54 for S, B, N3) with of more than one third of windows with D > 3 SDs from the mean (**Figure 2 – figure supplement 2**). However, most introgressed intervals are more spatially restricted. One locus of interest spanned an interval centered on *zyg11b* which has been implicated in craniofacial microsomia (**Figure 2E**)(Tingaud-Sequeira et

al., 2020). Another included multiple genes of interest including, *zswim*5, which is expressed in cranial neural crest (Wong et al., 2016), *rnf152*, which is involved in regulating neural crest formation (Yoon et al., 2022), and *mc4r*, which is a crucial regulator of appetite and metabolism via leptin and thyroid signaling modulation (**Figure 2F**)(Decherf et al., 2010). This suite of craniofacial and metabolic genes may have functioned like a supergene, which was spread via shared introgression among the Bigmouth and Nosed lineages and subsequently reinforced the differentiation of distinct lineages.

Patterns of differentiation between river and lake populations of Dolly Varden charr

To understand the shared variation that differentiates the Lake Kronotskoe residents from the river-caught anadromous population of Dolly Varden, pairwise Fst was calculated per coding (25,373 genes) and conserved non-coding element (CNE)(22,575 CNEs) from our targeted capture (**Figure 3A, B**). Fst values were computed by grouping all variation contained within the species flock and comparing against the variation contained in the riverine Dolly Varden charr population (lake versus river). There are 327 genes (**Supplementary File 3**) and 80 CNEs (**Supplementary File 4**) with Fst > 0.5. Each CNE was assigned to flanking target genes by GREAT (McLean et al., 2010). Some intervals harbor multiple highly differentiating CNEs. For example, the close proximity of two CNEs led to two hits for *cholinesterase-like* and *dync2h1* (**Figure 3B**). Interestingly, craniofacial (orange) and thyroid (blue) related genes (5 craniofacial genes of top 20, 2 thyroid genes of top 20) and CNEs (12 craniofacial CNEs of top 20, 3 thyroid CNEs of top 20) are well represented among the most differentiating elements (**Figure 3A, B**).

Craniofacial genes assigned to highly differentiating CNEs by GREAT analyses included both those with predicted roles in neural crest (*tfap2a*) (Rothstein & Simoes-Costa, 2020), as well as frontonasal (*meis2, pitx2*) (Evans & Gage, 2005; Fabik et al., 2020) and splanchnocranium (*faf1*) development (Ma et al., 2017). Of note, *pitx2* is also involved in release of thyroid stimulating hormone from the pituitary (Castinetti et al., 2011). *dync2h1* and *tfap2a* appear more than once in our analyses as putative regulated loci, suggesting multiple alterations to gene expression domains, timing, or strength at these loci may contribute to the genetic landscape that distinguishes the riverine Dolly Varden from the lacustrine morphs. Some CNEs are flanked on both sides by genes implicated in craniofacial development (*ofcc1* and *tfap2a*, *meis2* and *spred1*, *fam172a* and *nr2f1a*). Genes connected to ion transport (*myh6, khnyn, or11a1, endod1, cacnb2,* and *hrh1*), and vesicular transport (*man2a1, shld2, gdpd2, onecut2,* and *clint1a*) according to KEGG and Reactome reconstructions are also well represented among the top differentiating genes and as targets of the top differentiating CNEs. The majority of nucleotide changes identified were single SNPs with unknown functional significance. However the high Fst is reflective of potential selection or bottleneck at the locus. GO terms were assigned to all genes (2,825 GO terms) and CNEs (1,419 GO terms) that differentiate anadromous Dolly Varden from Lake Kronotskoe residents (Fst > 0.5). Among GO terms appearing 6 or more times, specific tendencies and themes emerged (**Fig. 3C**). Highly

differentiating genes are associated with roles in ion channel regulation and protein trafficking. Highly differentiating CNEs are associated with brain, kidney, and cartilage development. Other functions shared among highly differentiating coding and noncoding elements include functions such as DNA binding, transcription factors, and regulation of RNA polymerase II (**Supplementary file 5**).

Within the candidate genes, there are signals related to regulation of thyroid signaling in development. For example, the gene *slc26a10,* encoding a sulfate transporter, functions as a part of thyroid hormone synthesis, and acts downstream of thyroid hormone receptor alpha (Thra) (Richard et al., 2020). We found that *slc26a10* has segregating nonsynonymous changes in conserved residues that are highly differentiated between riverine and lacustrine morphs (**Figure 4A, B**). The function of this gene however is not well understood and alignment based analyses predict this amino acid substitution to have little effect on function (neutral by PROVEAN, tolerated by SIFT) (Choi & Chan, 2015; Ng & Henikoff, 2003). By Fst score, the next candiate gene, *catl1l,* encodes Cathepsin L1-like and is orthologous to cathepsin L1. This gene is predicted to contribute to normal function of the thyroid and have proteolytic functions which facilitate release of T4 from its prohormone thyroglobulin (Friedrichs et al., 2003). Next, splicing factor 3b subunit 4 (*sf3b4)* is a key developmental regulator of frontonasal patterning and growth and is associated with craniofacial Nager syndrome in humans (Bernier et al., 2012). Within this locus, we find synonymous variants at high Fst in all lacustrine morphs, and fixed within benthic groups (**Figure 5A, B**). These elevated footprints of clustered, highly differentiating variants may indicate the presence of further modifications within poorly conserved non-coding regions in linkage to these sites which were not targeted by our bait sequences.

Thyroid hormone signaling activity is associated with shifts in craniofacial form

As modulation of thyroid signaling has been implicated in charrs phenotypic specialization in different environments (E. V. Esin et al., 2021), the pattern of fixation in thyroid associated genes and non-coding elements in lacustrine morphs compared with riverine Dolly Varden warranted further investigation. To address if changes in thyroid signaling are associated with different morphs in Lake Kronotskoe, we assessed levels of circulating thyroid hormone in adult riverine and lacustrine individuals. Intriguingly, we found a significant decrease in T_3 hormone in specific lacustrine populations (**Figure 6A**). The pattern of reduced T_3 abundance across the species flock correlates with a clear change in craniofacial proportions: Nosed and Smallmouth morphs, with their subterminally positioned mouths, have significantly lower hormonal level compared to riverine Dolly Varden charr and the lacustrine White morph, which have comparatively 'wild-type' craniofacial form, as well as the piscivorous Longhead and deep-water benthivorous Bigmouth morphs, which are highly specialized (**Figure 1D**).

Our findings identify a disproportionate number of differentiated loci in Nosed lineages that are known to regulate thyroid signaling (**Fig. 6B**). We assessed specific mutations identified

as fixed or nearly fixed (Fst > 0.9) within Nosed morphs that differentiate them from Longhead or White morphs. A candidate locus that differentiates the low T_3 Nosed 1 and Nosed 3 morphs from the Longhead and White outgroups is a *leptin* homologue (**Fig. 6C**). All salmonids have two leptin A ohnologues derived from the shared salmonid whole genome duplication. LeptinA2 paralogues encode an N-terminal sequence extended by 66 amino acids compared to LeptinA1 or B orthologues within salmonids. The nonsynonymous change differentiating Nosed lineages lies within a conserved residue of the unique sequence of this Leptin paralogue. As Leptin hormone modulates thyroid activity and vice versa, both endocrine signaling pathways affect global metabolic activity in concert. Notably, *mc4r*, which shows evidence of allele sharing between the Bigmouth and Nosed lineages, serves as a relay through which leptin stimulates the thyroid axis, suggesting that these hormonal axes may be modulated at multiple levels in differentiated lineages (Decherf et al., 2010). Exogenous leptin and thyroid hormone treatments are associated with enlarged craniofacial dimensions marking an intriguing relationship between these pathways and Nosed lineage diversification (Copeland et al., 2011; Shkil et al., 2012; Yagasaki et al., 2003; Zimmermann-Belsing et al., 2003).

We also identified a highly differentiating variant within a conserved non-coding enhancer of *otx2b* (**Fig. 6D**). Nosed 1 and Nosed 3 morphs are fixed or nearly fixed for a variant allele which lies in a predicted *Pax1* transcription factor binding site. *otx2b* is involved in development of the skull as well as the anterior pituitary gland, which is a source of hormonal signals also involved in thyroid regulation (Bando et al., 2020; Diaczok et al., 2008). Due to the significant overlapping domains of *pax1* and *otx2* in the pharyngeal arches and the oral endoderm from which the pituitary gland arises, the differentiating variant identified provides a plausible regulatory shift associated with evolution of craniofacial morphology (Liu et al., 2013; Liu et al., 2020).

Discussion

Lake Kronotskoe harbors a unique radiation of Dolly Varden charr that provides a powerful new case study of the genetic and developmental foundations supporting vertebrate radiations. Our data redefine the evolutionary relationships among the lake morphs and supports differentiated true-breeding lineages. Previous models based on morphology, ecology and feeding behavior suggest two lacustrine clades: a deep-water clade consisting of Smallmouth and Bigmouth morphs, and a shallow-water clade composed of Longhead, White, and Nosed morphs (Markevich et al., 2018).

Lake Kronotskoe arose from a volcanogenic event and, presently drains via a waterfall which is considered impassable by charr (Viktorovskii, 1978). Pairwise Fst analyses found that each lake lineage is more differentiated from riverine Dolly Varden than from any other lineage. Furthermore, each lake lineage is differentiated from riverine Dolly Varden charr at roughly equivalent levels. We also determined that the Lake Kronotskoe lineages maintain reproductive isolation through low hybridization. By contrast, the much older Lake Malawi cichlid radiation,

has f-branch values commonly exceeding 5% and up to 14.2% (Malinsky et al., 2018) and *Coregonus* salmonids also have extensive introgression (De-Kayne et al., 2022b). These new data suggest that the species flock in Lake Kronotskoe was established by a single founding population having shared genetic signatures that quickly established and maintained thoroughly reproductively isolated populations.

We found specific genetic differentiation between lacustrine resident lineages and riverine Dolly Varden populations with selective signatures in genes regulating craniofacial development and thyroid function. While the relationship to morphological radiation is less clear, the abundance of ion transport and protein trafficking genes among the highly differentiating genes, suggests that these processes may also be important drivers of charr evolution. Crucially, ion homeostasis is central to effective osmoregulation during freshwater adaptation (S. D. McCormick et al., 2019). Whether and how vesicular function contributes to adaptations in Lake Kronotskoe is less obvious. Differentiating CNEs are associated with roles in brain, kidney, and cartilage development. The kidneys are indispensable for osmoregulation and obligate freshwater populations of salmonids place different demands on their kidneys their anadromous counterparts (Tipsmark et al., 2010). Cartilage templates lay foundations for most craniofacial structures. The data suggest that CNEs are particularly influential in the evolution of kidney function and cartilage morphology within the Lake Kronotskoe radiation. Additionally, genes that function in thyroid hormone regulation are differentially selected, suggesting modulation of the hormone may underlie stereotypical phenotypic shifts in lacustrine charr morphology. It is important to note that while PROVEAN and SIFT predicted the serine substitution shared among the lake morphs would have little consequence upon *slc26a10* function, such alignment based prediction methods would tend to underestimate potential effects if variation is shared in other lineages (Choi & Chan, 2015; Ng & Henikoff, 2003). Indeed, the multiple sequence alignment showed that zebrafish also encode serine at that residue. As many specialized morphologies are hypothesized to arise from heterochronic shifts in development (Simonsen et al., 2017), the thyroid axis may prove to be a common mechanism underlying the adaptive potential and may contribute to the remarkable similarity of morphologies exhibited by lacustrine charr species flocks (E. V. Esin et al., 2021; Evgeny V. Esin, Grigorii N. Markevich, Dmitriy V. Zlenko, et al., 2021). Indeed, the pairs of morphs in each of the Lake Kronotskoe clades exhibit alternative heterochronic tendencies. For example, the Smallmouth morph with proportionally large eyes and blunt, rounded rostra shows hallmarks of paedomorphosis, while the sister Bigmouth morph possesses peramorphic traits such as overdeveloped lower jaw. The enlarged jaws and frontonasal protrusion of the Longhead morph, as well as the drastically modulated frontonasal proportion of the Nosed 3 morph are peramorphic features in comparison to their sister lineages. Similar craniofacial adaptive changes arose during the adaptive radiation of phylogenetically distant fishes, the large African barbs (g. *Labeobarbus*; Cypriniformes; Teleostei), inhabiting Lake Tana (Nagelkerke & Sibbing,

2000). The age of the Lake Tana species flock of barbs is comparable with the Lake Kronotskoe species flock, yet genetic differences between Lake Tana morphs are comparatively subtle (de Graaf et al., 2010; Nagelkerke et al., 2015), and ecomorphological differentiation is a result of heterochronic shifts presumably induced by thyroid axis alterations (Shkil et al., 2015).

Such similarities suggest that genetic modification of thyroid signaling may be a widespread mechanism facilitating rapid freshwater teleost adaptive radiations and provide a genetic foundation from which more specialized morphologies may be further elaborated.

In anadromous salmonids, smoltification in preparing for migration out to sea requires orchestration of hormonal and physiological switches. A hypothesis stemming from lacustrine populations is that selective pressure on the ancestral riverine charr population was relaxed upon colonization of the lake, as the newly resident population of charr became obligate freshwater residents. Such an initial initial shift in developmental programs may constitute a common node among lacustrine-locked charr which biases the direction of adaptation to generate similar forms among independent lineages, thereby laying the foundation upon which more trophically specialized morphologies may arise. In this context, exclusion of the smoltification stage from the charr life cycle may permit lacustrine adaptive diversification.

Endocrine signaling pathways, including the growth, hypothalamic-pituitary-interrenal, and thyroid axes drive physiological, morphological, and behavioral changes during smoltification (McCormick, 2012). In landlocked salmonid populations, the growth and hypothalamic-pituitary-interrenal axes, which ordinarily induce physiological changes for a transition to seawater, are upregulated, while the thyroid axis likely maintains its developmental, physiological, and adaptive significance (Stephen D. McCormick et al., 2019). In support of this model, thyroid hormone signaling is selectively modified during freshwater colonization and subsequent adaptive radiations of the threespine stickleback, *Gasterosteus aculeatus* (Kitano et al., 2010).

The lineage-specific pattern of highly differentiating loci identified in Nosed morphs, suggests that an initial developmental state of extensive modifications to thyroid signaling and craniofacial development shared among all lineages, was further refined in these lineages. The fixation of variation in *leptina2* and a predicted *otx2b* regulatory region found in Nosed morphs over other lake groups suggests further modulation to the thyroid axis in these lineages. The data are supported by findings of altered T_3 levels within these lineages as adults and the presence of *mc4r* within an interval of excess allele sharing with the Bigmouth morph. Thus, beginning with an initial suite of shared genetic variants, lineage-specific, secondary elaborations may have further catalyzed the exceptional species flock diversification in Lake Kronotskoe.

Such repeated and parallel derivations of morphotypes across the *Salvelinus* complex suggest that there is an underlying genetic framework biasing the radiations of resident lacustrine populations. Our data suggest that shared modulation of the thyroid signaling axis in

tandem with craniofacial regulators may enforce such biases. The patterns of variation identified in the Lake Kronotskoe radiation point to a fundamental genetic groundwork for craniofacial evolution and a common axis for morphological change. Our genomic data and description of this unique radiation opens the door for systematic in-depth studies of the genetic roots of morphological evolution.

Methods

Field material collection

Charrs that passes the spawning season, adults without spawning changes in color and head and reproductive states, were sampled in Lake Kronotskoe. Adult riverine Dolly Varden charrs were collected in the nearest watercourse draining the opposing slope of Valaginskiy range. Blood, pectoral fin tissue and pictures were collected. Blood for thyroid hormone test was carefully collected from the caudal vessel with a Vacuette serum tube. The distal part of the right pectoral fin (finclip, 0.2-0.3 cm^2) was taken with scissors and fixed in pure alcohol for DNA analysis. Fish were photographed, treated with the antibacterial and antifungal solution (Melafix and Pimafix, API) for 30 min, and released if the fish did not display any signs of injury and/or infection in 48 hrs. All catches were carried out in accordance with the Russian Federal Act on Specially Protected Natural Areas (OOPT) N33-ФЗ 14/03/1995, article 10, and Plan of the research activities of Kronotsky Nature Reserve. The procedures with fish were approved by the Bioethics Commission of the AN Severtsov Institute of Ecology and Evolution, Russian Academy of Science.

Phylochip targeted sequence enrichment design

We aimed to create a pan-Salmoniformes targeted sequence capture design that can enrich sequencing libraries for conserved genetic regions across a broad diversity of available salmon genomes. This design targets protein-coding exons as well as a set of conserved non-protein coding elements (CNEs), miRNA hairpins, and ultraconservative non-coding elements (UCNEs). The majority of capture baits were derived from the Atlantic salmon genome (*Salmo salar*, ICSASG_v2)(Davidson et al., 2010), with inclusion of regions from the genome of rainbow trout (*Oncorhynchus mykiss*, AUL_PRJEB4421_v1)(Berthelot et al., 2014) that were either not represented in the Atlantic salmon genome or were <85% identity to a capture target within the rainbow trout genome. As these fish bracket both sides of the salmon phylogeny (**Supp. Fig. 1A**), the 'Phylochip' design strategy enables DNA from the majority of salmonids target regions to be efficiently enriched using this one capture design.

As the Atlantic salmon genome was not annotated at the time of capture design, annotated coding sequences were isolated from the rainbow trout and northern pike (*Esox lucius*, GCF_000721915.2_ASM72191v2)(Rondeau et al., 2014) genomes. These were then identified within the Atlantic salmon genome via BLASTN (ncbi-blast-2.2.30+; parameters '-max_target_seqs 1 -outfmt 6'), and these hits used in the capture design. Genes from rainbow trout that were not identified in Atlantic salmon or that had <85% identity to the best BLAST hit

within the Atlantic salmon genome were also retained in the capture design. CNEs were defined from the constrained regions in the Ensembl compara 11-way teleost alignment (Ensembl release-84)(Herrero et al., 2016). To reserve space in the capture design, only CNEs ≥75bp in length were included in the capture baits. These CNEs were extracted from the Japanese medaka (*Oryzias latipes*, MEDAKA1), three-spined stickleback (*Gasterosteus aculeatus*, BRAOD S1), and zebrafish (*Danio rerio*, GRCz10.84) genomes using Bedtools (v2.23.0) intersectBed (Aaron R. Quinlan & Ira M. Hall, 2010). miRNA hairpins were extracted from miRbase and ultraconservative elements (UCNEs) from UCNEbase (Dimitrieva & Bucher, 2013; Kozomara & Griffiths-Jones, 2010). As with protein coding exons, these elements were identified within each reference genome using BLASTN (ncbi-blast-2.2.30+; parameters '-max_target_seqs 1 -outfmt 6'). miRNA hairpins were padded to be at least 100 bp to improve capture specificity.

From these targeted regions, the specific SeqCap EZ Developer (cat #06471684001) oligonucleotide capture baits were made in collaboration with the Nimblegen design team. Capture baits are strategically designed to standardize oligo annealing temperature, remove low complexity DNA regions and to reduce the oligo sequence redundancy. The capture design targeted sequence from 558,882 genomic regions (97,049,118 total bp) across the two salmonid genomes. This included including 460,210 protein coding exons, 93,973 CNEs, 1,082 miRNAs and 3,617 UCNEs (**Supp. Fig. 1**).

DNA extraction and preparation of sequencing libraries

Tissue from finclips was digested and genomic DNA was column purified using QIAGEN DNeasy Blood & Tissue Kit (QIAGEN 69506). Genomic DNA was extracted from finclips of 1 *S. leucomae*nis, 3 riverine Dolly Varden charr, 8 Bigmouth morphs, 10 Longhead morphs, 5 Nosed1 morphs, 7 Nosed2 morphs, 5 Nosed3 morphs, 6 Smallmouth morphs, and 6 White morphs. Pools of genomic DNA were produced for each lineage such that genomic DNA from every individual in a lineage pool was equally represented. The pooled samples were sheared to a target size of 200bp in Tris-HCl EDTA shearing buffer (10mM Tris-HCl, 0.1mM EDTA, pH 8.0). Mechanical shearing was performed using a Covaris E220 ultrasonicator (duty cycle, 10%; intensity, 5; cycles/burst, 200; time, 400 seconds; temperature, 8°C) and Covaris microTUBE Snap-Cap tubes (Covaris 520045). Sequencing libraries were produced using the KAPA HyperPrep Kit (Roche 07137923001) using 500ng of starting material for each library. Library preparation was conducted by following the SeqCap EZ HyperCap Workflow Version 1.2. The sequencing library for the Nosed2 samples utilized enzymatic shearing using the KAPA HyperPlus Kit (Roche 07962401001) and 100ng of starting material (SeqCap EZ HyperCap Workflow Version 3.0). Fragment size and DNA concentration were quantified using Agilent 2100 BioAnalyzer and High Sensitivity DNA Chips (Agilent 5067-4626). Paired-end, 150bp Illumina HiSeq sequencing was performed on a pool consisting of multiple barcoded libraries.

Trimming Adapters and Read Mapping

Illumina adapter sequences were removed from reads using Trimmomatic v0.36 (Bolger et al., 2014). Trimmed and masked reads were aligned to the *Salvelinus alpinus* reference genome (RefSeq Assembly accession: GCF_002910315.2) using NextGenMap v0.5.5 (Sedlazeck et al., 2013). The flag - - strata 1 was so only the highest scoring read mappings were recorded in the alignment file.

Variant Calling and Filtering

The variants used to reconstruct the phylogeny and to conduct the principal components analyses were derived from sample of *S. leucomaenis*, anadromous Dolly Varden, and all 7 members of the species flock. samtools v1.15.1 was used to fix mates, mark duplicates, and filter reads below the minimum mapping quality set to -q 30 (Danecek et al., 2021). bcftools v1.13 was used to call and filter variants (Danecek et al., 2021). Only the variants with quality scores >= 20, depth of coverage on a per-sample basis between 10 and 500 reads, fraction of missing genotypes F_MISSING <= 0.72. SNPs within 2bp of indels and other variant types were excluded, and minor allele frequency > 0.05. The quality filtered VCF file contained 623,619 variants. The set of variants used for introgression analyses, quantification of Fst, π, and GOterm enrichment analyses were called and filtered from alignments of the anadromous Dolly Varden, Bigmouth, Longhead, Nosed 1, Nosed 3, Smallmouth, and White lineages (*S. leucomaenis*, and Nosed 2 were excluded). The calling and filtering criteria are identical to the conditions described above except for the depth thresholds. Those were filtered on a per site basis for coverage between 70 and 3500 reads. This VCF file contained 526,811 variants.

Coverage of Targeted elements

Coverage statistics were derived using the BEDTools v2.21.1 coverage function (A. R. Quinlan & I. M. Hall, 2010). Alignment files were intersected with a bed file containing the positions of each targeted element. From this intersection, the average depth of coverage was quantified per base.

Deriving Phylogeny

The phylogeny was derived using IQ-TREE v1.6.12 (Nguyen et al., 2015) . The input consisted of 622,831 nucleotide sites, including 22,701 parsimony informative variants. The ModelFinder function (Kalyaanamoorthy et al., 2017) determined the base substitution model of best fit to be a transversion model with empirical base frequencies and a proportion of invariable sites (TVM + F + I). 1,000 ultrafast bootstrap replicates (Hoang et al., 2017) quantified support for the phylogeny.

Principal Components Analysis

PLINK v1.90b7 was utilized to conduct principal components analysis (Purcell et al., 2007). Linkage pruning was conducted using 50kb windows, 10bp step size, and $R^2 > 0.1$. The linkage pruned dataset consisted of 65,488 variant sites. The PLINK eigenvector and eigenvalue outputs were plotted in R.

Introgression Analysis

Introgression was quantified for all trios in the phylogeny using Dsuite v0.4 (Malinsky et al., 2021) Dtrios. Riverine Dolly Varden was specified as the outgroup. The f-branch statistic was depicted as a matrix by taking the output from Dsuite Fbranch and running the Dsuite dtools.py script to generate a plot. Dinvestigate was used to generate sliding windows of 40 variants per window and 50% overlap.

Calculating pairwise Fst and Tajima's Pi

To quantify genetic differentiation, pairwise Fst was calculated using PoPoolation2 v1201 (Kofler, Pandey, et al., 2011). The software package allows Fst to be quantified in sliding windows or in a genewise manner. Sequencing alignment data were converted into the mpileup format using SAMtools v1.13 (Li et al., 2009). The PoPoolation2 program mpileup2sync (--min-qual 20) generated the sync file used as input to calculate Fst in sliding windows. Popoolation2 calculated Fst based on allele frequency (Hartl et al., 1997). The PoPoolation2 program fst-sliding (--min-coverage 20 --min-count 3 --max-coverage 200) was used to calculate Fst in non-overlapping sliding windows. To assess which genes were most differentiating between populations, the function create-genewise-sync was utilized to intersect the sync file with a gtf containing all targeted regions in the *S. alpinus* genome, and filtered according to the same depth and minor allele count criteria as sliding windows analyses. Prior to filtering for depth, Fst was calculated for 59,478 genes and 22,590 CNEs. Noncoding elements were associated with putative regulatory targets by following the GREAT workflow to establish basal regulatory windows. A BED file of CNE loci was intersected with Intervals spanning 5kb upstream of and 1kb downstream from transcriptional start sites, with up to a 1 Mb extension (McLean et al., 2010). To quantify nucleotide diversity, Tajima's Pi was calculated using PoPoolation v1.2.2 (Kofler, Orozco-terWengel, et al., 2011). The software also enables quantification of Tajima's Pi in sliding windows. The same depth criteria that were used for Fst sliding window quantifications were used to calculate Tajima's Pi in sliding windows for individual lineages.

Elisa for Thyroid hormone in blood

Serum samples were transferred to 2 ml specimen tubes and centrifuged at 12 000 g for 10 min with Eppendorf MiniSpin. Serum was then collected into Eppendorf 1.5 ml tubes and placed in in freezer at 24-26C. The total triiodothyronine (T3, bioactive form of thyroid hormone)

concentration in plasma was evaluated by enzyme-linked immunosorbent assay (Monobind Total Triiodothyronine (tT3) test system, Monobind Inc, USA) and measured the hormone in accordance with the manufacture protocol using StatFax 303 Plus strip reader (Awareness Technology Inc, USA).

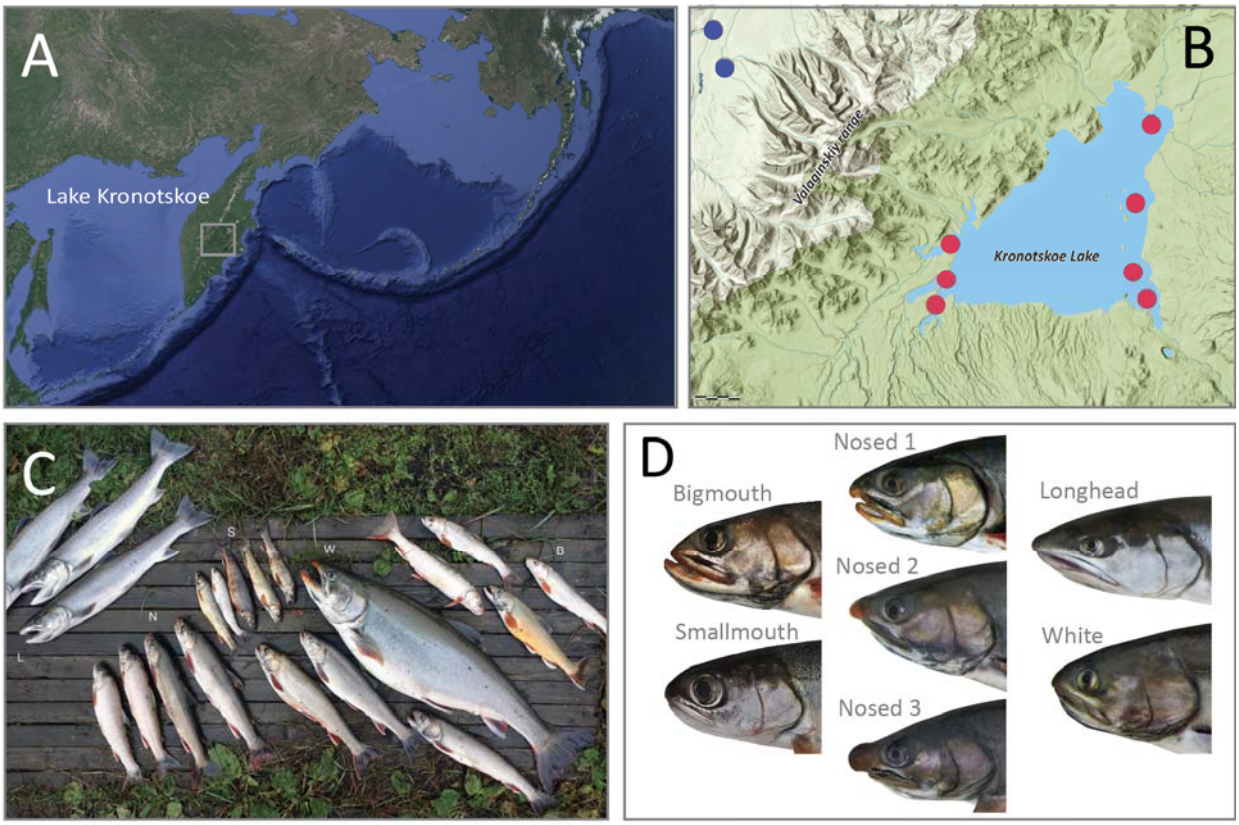

Figure 1. Lake Kronotskoe radiation of Dolly Varden Charr. (A) A map of the Kamchatka Peninsula. Lake Kronotskoe is centered within the highlighted box. **(B)** A map of Lake Kronotskoe geography and locations from which anadromous (blue dots) and resident lacustrine (red dots) Dolly Varden morphs were collected. **(C)** The Lake Kronotskoe morphs from left to right: Longhead (L), Nosed lineages (N), Smallmouth (S), White (W), Bigmouth (B). **(D)** Detailed images of representative adult heads for the seven sequenced lineages of the species flock.

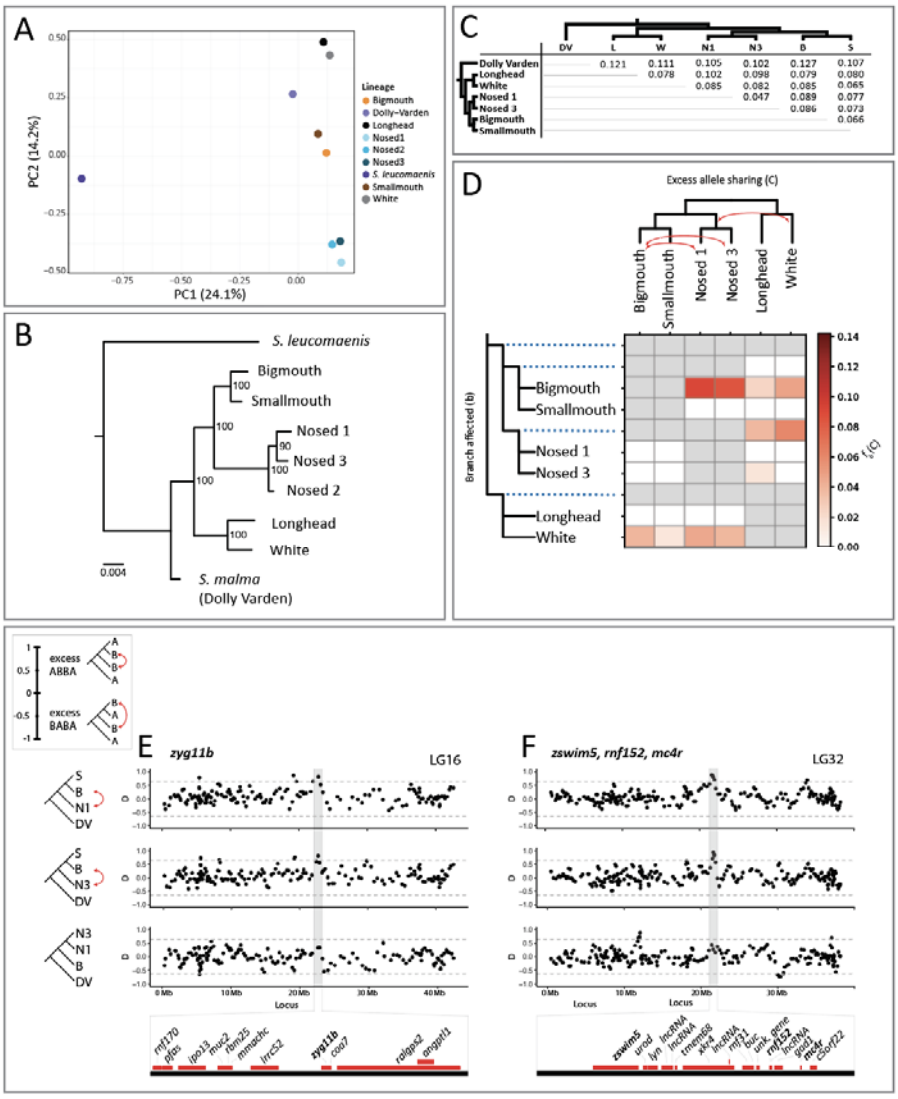

Figure 2. Phylogenetics and population differentiation among the sequenced lineages. (A) PCA plot of the seven lineages from the lacustrine species flock, and outgroups anadromous Dolly Varden and *S. leucomaenis*. PC1 distinguishes *S. Leucomaenis* from anadromous Dolly Varden and from the lake morphs. Note the tight clustering of the three Nosed morphs. **(B)** Phylogenic relationship of Lake Kronotskoe Dolly Varden lineages; anadromous *S. leucomaenis* from the Kamchatka River serve as the outgroup. **(C)** Distribution of genome-wide, pairwise Fst values calculated for non-overlapping 10kb sliding windows (**Supplementary File 5**). **(D)** The branch-specific statistic f_b shows evidence for elevated gene flow between the Bigmouth and Nosed 1 morphs, the Bigmouth and Nosed 3 morphs, and the ancestor of the Nosed lineages and the White morph. White cells represent combinations for which p-values are not significant. Gray cells represent arrangements which are not topologically feasible for calculating *f*-branch scores. **(E)** Sliding window plots of D for trios consisting of Smallmouth (S), Bigmouth (B), and Nosed 1 (N1), of S, B, and Nosed 3 (N3), and of N3, N1, and B. Positive D values indicate an excess of the ABBA pattern (red arrows), while negative values indicate an

excess of the BABA pattern. The three plots show a common pattern of excess of allele sharing overlapping with *zyg11b* between B and N1 and B and N3, while there is no excess of allele sharing between B and N1 over B and N3. Horizontal lines signify 3SDs from the mean. Genes contained by the highlighted peak represented by red bars below plots. **(F)** three genes of interest, *zswim5*, *rnf152*, and *mc4r*, possibly constitute a supergene contained by a shared peak between B and N1 and B and N3.

Figure 2 – Supplementary Figure 1. Design of pan-Salmoniformes targeted capture array. (A) Conserved bait sequences were derived from Atlantic salmon (*Salmo salar*) and rainbow trout (*Oncorhynchus mykiss*) reference genomes. **(B)** Relative contributions of *S. salar* and *O. mykiss* derived bait sequences to the capture array. **(C)** Classifications and relative abundances of conserved elements targeted for capture.

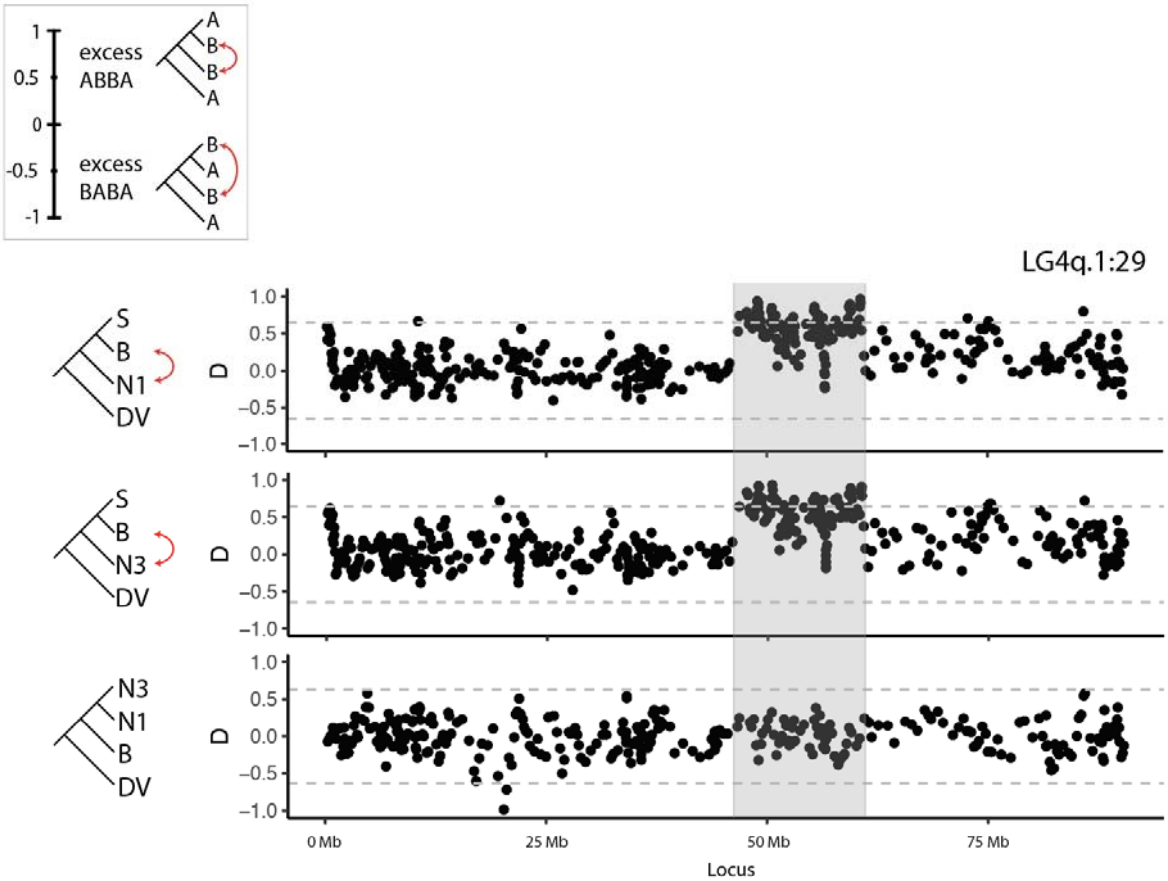

Figure 2 – Supplementary Figure 2. Sliding window plots of D showing a *large* interval of excess allele sharing. Sliding window plots for trios consisting of Smallmouth (S), Bigmouth (B), and Nosed 1 (N1), of S, B, and Nosed 3 (N3), and of N3, N1, and B. Positive D values indicate an excess of the ABBA pattern (red arrows), while negative values indicate an excess of the BABA pattern. The three plots show a common pattern of excess of allele sharing overlapping with between B and N1 and B and N3, while there is no excess of allele sharing between B and N1 over B and N3. Horizontal lines signify 3SDs from the mean.

Morphotype	No. Individuals Pooled	No. Reads (million)	No. Reads Mapped	Median Depth	Mean Depth	"Conservome" Coverage 2x	"Conservome" Coverage 10x
Bigmouth	8	72.3	35.3	66 reads	88 reads	91.6%	88.5%
Dolly Varden	3	64.1	32.4	61 reads	82 reads	91.6%	88.3%
Longhead	10	46.1	22.8	41 reads	56 reads	91.1%	85.7%
Nosed 1	5	68.8	34.9	65 reads	87 reads	91.7%	88.5%
Nosed 2	7	49.5	17.5	16 reads	20 reads	88.7%	65.5%
Nosed 3	5	68.4	34.1	63 reads	84 reads	91.6%	88.5%
Smallmouth	6	43.1	21.1	38 reads	52 reads	90.8%	84.9%
S. leucomaenis	1	55.9	25.5	50 reads	67 reads	90.5%	85.9%
White	6	36.9	18.5	34 reads	46 reads	90.6%	83.8%

Figure 2 – Supplementary Table 1. Summary of reads aligned and targeted element coverage.

GO name	GO accession	bin size
activation of MAPK activity	GO:0000187	15
anaphase-promoting complex	GO:0005680	51
anaphase-promoting complex-dependent catabolic process	GO:0031145	41
ATP-dependent chromatin remodeling	GO:0043044	133
ATPase activity	GO:0016887	262
calcium ion binding	GO:0005509	1185
calcium, potassium:sodium antiporter activity	GO:0008273	52
carbohydrate binding	GO:0030246	111
carbohydrate metabolic process	GO:0005975	204
cell adhesion	GO:0007155	541
chemokine activity	GO:0008009	72
cullin-RING ubiquitin ligase complex	GO:0031461	23
DNA binding	GO:0003677	2972
DNA integration	GO:0015074	1571
DNA-templated transcription, initiation	GO:0006352	36
ferric iron binding	GO:0008199	24
fructose-bisphosphate aldolase activity	GO:0004332	27
hexose metabolic process	GO:0019318	34
homophilic cell adhesion via plasma membrane adhesion molecules	GO:0007156	362
iron ion transport	GO:0006826	23
isomerase activity	GO:0016853	45
MAP kinase activity	GO:0004707	52
nucleic acid binding	GO:0003676	2731
oligopeptide transport	GO:0006857	20
phosphatidylinositol metabolic process	GO:0046488	49
phosphatidylinositol phosphate kinase activity	GO:0016307	47
receptor tyrosine kinase binding	GO:0030971	28
regulation of mitotic metaphase/anaphase transition	GO:0030071	44
sensory perception of sound	GO:0007605	69
skeletal muscle fiber development	GO:0048741	44
SWI/SNF complex	GO:0016514	147
transcription coactivator activity	GO:0003713	164
transcription factor TFIID complex	GO:0005669	38
transmembrane transport	GO:0055085	1148
transmembrane transporter activity	GO:0022857	306
transporter activity	GO:0005215	218
transposition, DNA-mediated	GO:0006313	1551
ubiquitin protein ligase binding	GO:0031625	28
vesicle-mediated transport	GO:0016192	250

Figure 2 – Supplementary Table 2. Table of significantly underrepresented GO terms. This table contains the set of significantly underrepresented GO terms among all sample libraries (Benjamini-Hochberg FDR < 0.05).

Pop 1	Pop 2	Pop 3	D_{tree} (%)	f_4-ratio (%)	p-value	Z-score
S	N3	W	3.9	8.6	0	13.0*
S	N1	W	3.7	8.2	0	11.4*
S	N3	L	2.8	6.3	0	11.4*
S	N1	L	2.2	4.9	1.18E-16	8.3*
S	B	N1	4.2	9.0	1.56E-15	8.0*
S	B	W	2.2	4.7	1.26E-14	7.7*
B	N3	W	1.8	4.1	2.44E-14	7.6*
L	W	N1	2.2	4.5	2.73E-13	7.3*
L	W	B	1.7	3.9	2.76E-13	7.3*
B	N1	W	1.7	3.7	2.11E-12	7.0*
S	B	N3	3.6	8.3	2.31E-11	6.7*
L	W	N3	1.8	3.8	4.65E-09	5.9*
B	N3	L	1.8	4.0	6.52E-07	5.0*
S	B	L	1.1	2.4	1.01E-04	3.9*
B	N1	L	1.2	2.6	3.59E-04	3.6*
N1	N3	L	0.7	1.5	1.13E-03	3.3*
L	W	S	0.5	1.4	2.86E-03	3.0
N1	N3	S	0.4	0.9	5.72E-02	1.9
N1	N3	W	0.2	0.5	2.79E-01	1.1
N3	N1	B	0.3	0.7	2.86E-01	1.1

Figure 2 – Supplementary Table 3. Table of D_{tree} scores, f_4-admixture ratios, and Z-scores for each of the 20 trios contained within the Lake Kronotskoe species flock. 16 trios were found to have a significant, though minimal, contribution of introgressed alleles (asterisks)(Holm-Bonferoni, FWER < 0.01). B, Bigmouth; L, Longhead; N1, Nosed 1; N3, Nosed 3; S, Smallmouth; W, White.

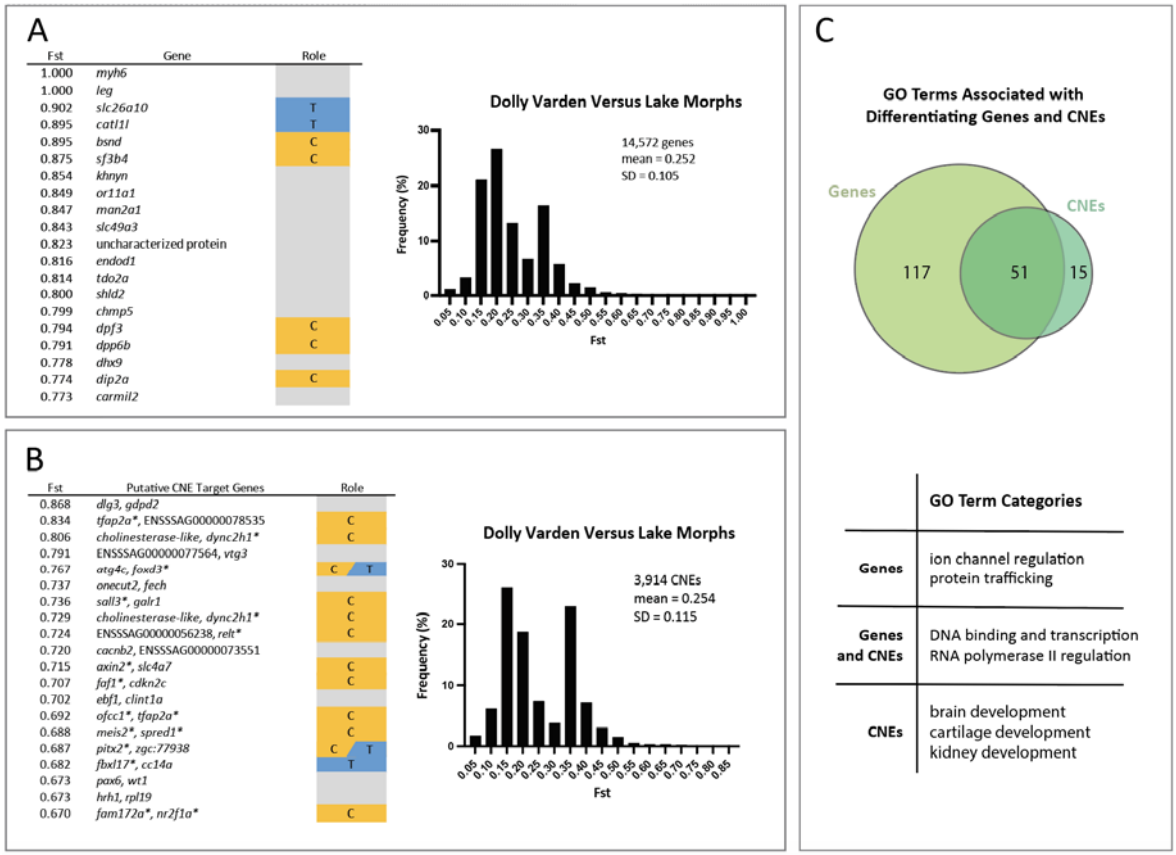

Figure 3. Coding and non-coding conserved elements differentiating anadromous Dolly Varden charr from the Lake Kronotskoe species flock. A) Table showing the top 20 genes differentiating riverine Dolly Varden from Lake Kronotskoe inhabitants along with distribution of Ft values of genes. B) Table of the top 20 differentiating CNEs and the distribution of Fst values. C) Overview of shared and unique GO terms associated with genes and CNEs with Fst > 0.5. Venn diagram values represent GO terms which occur six or more times. Table summarizes broad categories of most frequent GO term associations. The distributions and the numbers of elements represent all non-zero Fst values; *orange*, genes with known roles in modulating craniofacial morphology (C); *blue*, genes with known roles in thyroid function (T). Asterisk denotes gene classified as (C), (T), or both.

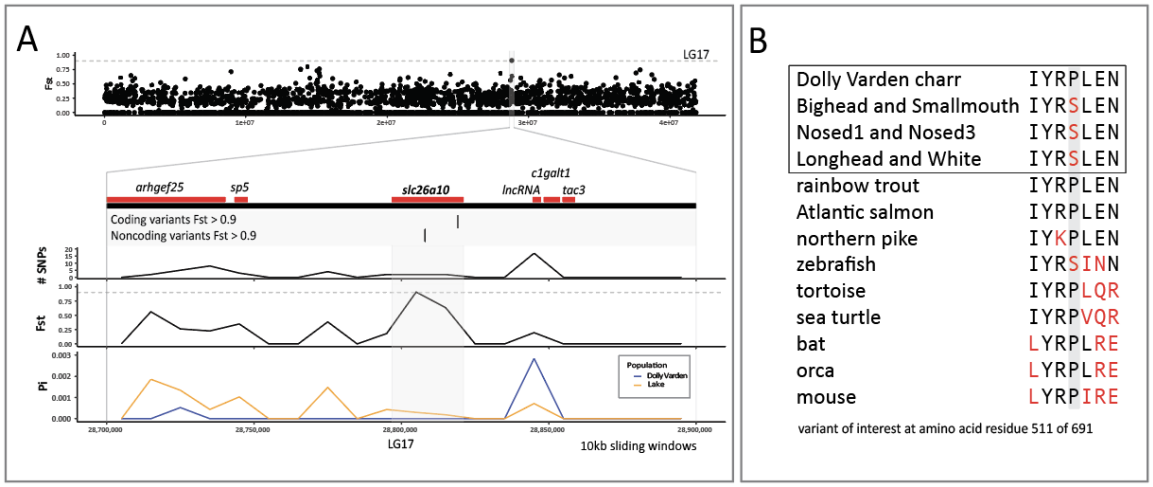

Figure 4. Differentiation of *slc26a10* in pairwise comparisons between anadromous Dolly Varden charr and the Lake Kronotskoe species flock. (A) The *slc26a10* locus shows high differentiation (Fst). The gene locus contains one highly differentiating non-coding and one coding variant. Dolly Varden *slc26a10* is homologous to human pendrin (*SLC26A4*), a known thyroid regulator. The broader locus has low nucleotide diversity as illustrated by sliding window plots of Tajima's Pi. Horizontal dotted gray line represents Fst = 0.9. Plots are included for 10kb sliding windows along LG17, the coding elements within the broader locus, the number of variants per sliding window, Fst, and Tajima's Pi per sliding window in pairwise comparisons between riverine Dolly Varden charr and the Lake Kronotskoe species flock. **(B)** Slc26a10 contains a fixed amino acid substitution in a conserved proline that differentiates Dolly Varden charr from each of the major clades of the lacustrine morphs.

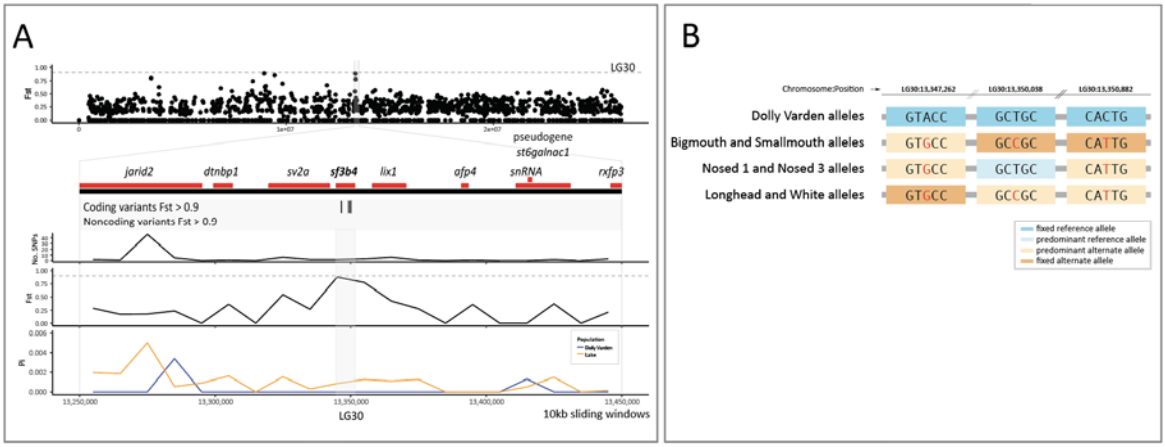

Figure 5. Fixation of variation in s*f3b4* between anadromous Dolly Varden charr and the Lake Kronotskoe species flock. **(A)** Three highly differentiating synonymous variants lie within *sf3b4*. Fst is plotted in non-overlapping 10kb sliding windows along the length of the chromosome LG30. *Sf3b4* is contained within a 200kb interval of low nucleotide diversity as illustrated by sliding window plots of Tajima's Pi. Horizontal dotted gray line represents Fst = 0.9. The broad locus encompassing *sf3b4* is shown in detail including plots of the number of variants, Fst, and Tajima's Pi in 10kb non-overlapping sliding windows. **(B)** 3 synonymous variants in *sf3b4* are fixed in lacustrine Dolly Varden charr; *dark orange,* non-reference allele fixed*; light orange,* non-reference allele predominant (alt. allele freq. > 50%) in sequence pool; *Light blue*, a lineage for which the reference allele is predominant (ref. allele freq. > 50%) at the locus.

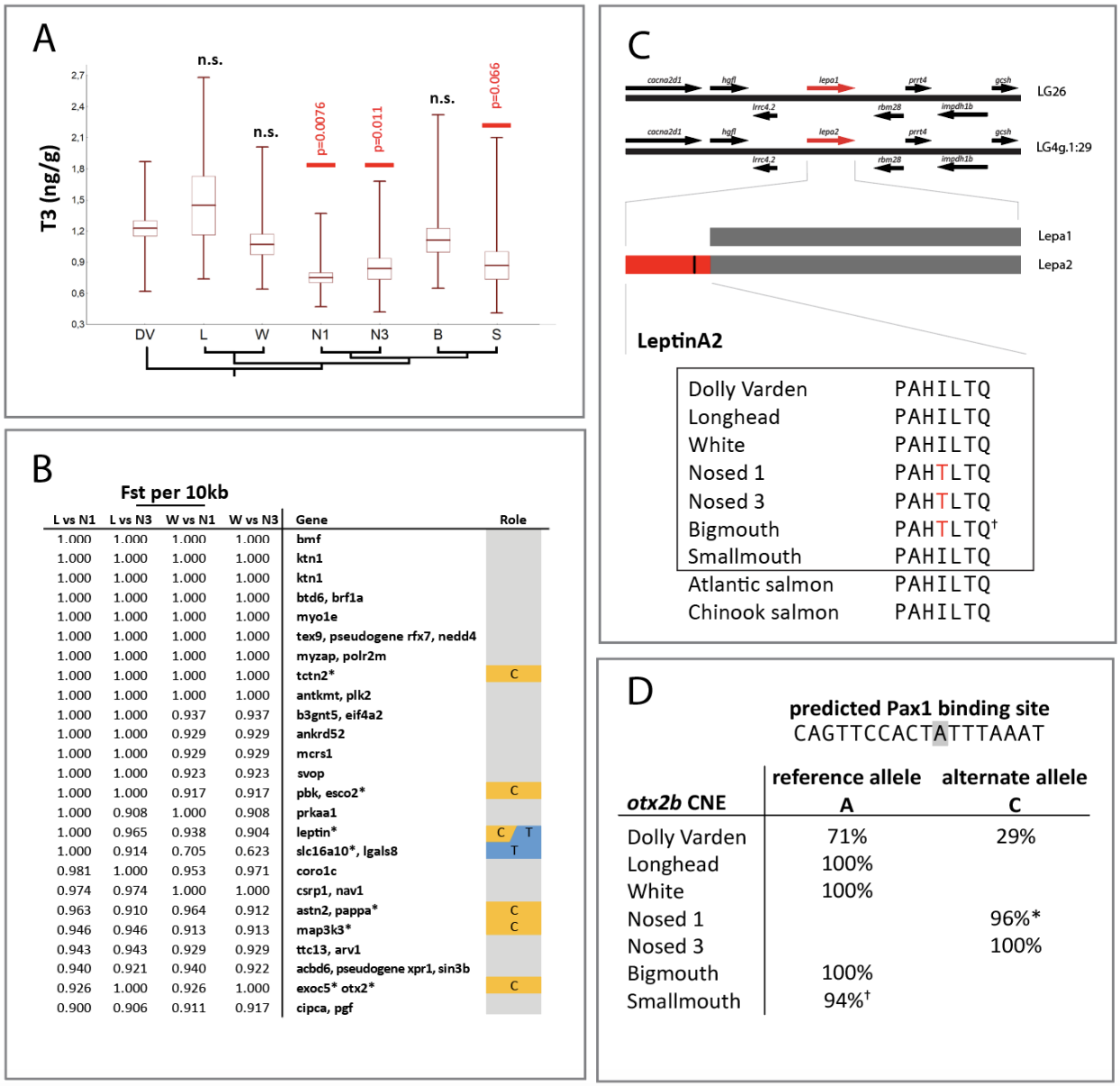

Figure 6. Thyroid hormone (T3) levels and associating highly differentiating candidates in lacustrine Dolly Varden morphs related to thyroid function and craniofacial morphology. **(A)** Serum T3 levels were significantly less in Nosed 1, Nosed 3, and Smallmouth lineages relative to anadromous Dolly Varden; mean +/- 1 SD, with boundary values indicated (min/max). **(B)** Top 20 candidate regions differentiating Nosed lineages from Longhead and White lineages. Sites uniquely differentiating Longhead morphs from Nosed 1 and Nosed 3 morphs, and White morphs from Nosed 1 and Nosed 3 morphs identify loci associated with thyroid function (blue, T) or craniofacial developmental (orange, C) modulating elements. **(C)** Schematic of Leptin A paralogues in salmonids detailing previously unknown gene *leptin a2* having a unique 66 amino acid N-terminus extension compared to its paralogues. Nosed lineages contain a fixed, non-synonymous SNP in this conserved N-terminal sequence. (**D**) An *otx2b* CNE contains fixed or

highly differentiating variants within a predicted Pax1 binding domain that associates with lake morphs exhibiting significantly different thyroid signaling activities; percentage of reference and alternate allele reads indicated per morph. Low level detection of variant or reference alleles noted (1 read for reference allele (asterisk), 2 reads for non-reference allele (dagger)).

References

Bando, H., Gergics, P., Bohnsack, B. L., Toolan, K. P., Richter, C. E., Shavit, J. A., & Camper, S. A. (2020). Otx2b mutant zebrafish have pituitary, eye and mandible defects that model mammalian disease. *Human Molecular Genetics*, *29*(10), 1648-1657. https://doi.org/10.1093/hmg/ddaa064

Barluenga, M., Stölting, K. N., Salzburger, W., Muschick, M., & Meyer, A. (2006). Sympatric speciation in Nicaraguan crater lake cichlid fish. *Nature*, *439*(7077), 719-723. https://doi.org/10.1038/nature04325

Bernier, F. P., Caluseriu, O., Ng, S., Schwartzentruber, J., Buckingham, K. J., Innes, A. M., Jabs, E. W., Innis, J. W., Schuette, J. L., Gorski, J. L., Byers, P. H., Andelfinger, G., Siu, V., Lauzon, J., Fernandez, B. A., McMillin, M., Scott, R. H., Racher, H., Consortium, F. C., . . . Parboosingh, J. S. (2012). Haploinsufficiency of SF3B4, a component of the pre-mRNA spliceosomal complex, causes Nager syndrome. *American journal of human genetics*, *90*(5), 925-933. https://doi.org/10.1016/j.ajhg.2012.04.004

Berthelot, C., Brunet, F., Chalopin, D., Juanchich, A., Bernard, M., Noël, B., Bento, P., Da Silva, C., Labadie, K., Alberti, A., Aury, J.-M., Louis, A., Dehais, P., Bardou, P., Montfort, J., Klopp, C., Cabau, C., Gaspin, C., Thorgaard, G. H., . . . Guiguen, Y. (2014). The rainbow trout genome provides novel insights into evolution after whole-genome duplication in vertebrates. *Nature Communications*, *5*(1), 3657. https://doi.org/10.1038/ncomms4657

Bolger, A. M., Lohse, M., & Usadel, B. (2014). Trimmomatic: a flexible trimmer for Illumina sequence data. *Bioinformatics*, *30*(15), 2114-2120. https://doi.org/10.1093/bioinformatics/btu170

Braitseva, O. A., Melekestsev, I. V., Ponomareva, V. V., & Sulerzhitsky, L. D. (1995). Ages of calderas, large explosive craters and active volcanoes in the Kuril-Kamchatka region, Russia. *Bulletin of Volcanology*, *57*(6), 383-402. https://doi.org/10.1007/BF00300984

Castinetti, F., Brinkmeier, M. L., Gordon, D. F., Vella, K. R., Kerr, J. M., Mortensen, A. H., Hollenberg, A., Brue, T., Ridgway, E. C., & Camper, S. A. (2011). PITX2 and PITX1 Regulate Thyrotroph Function and Response to Hypothyroidism. *Molecular Endocrinology*, *25*(11), 1950-1960. https://doi.org/10.1210/me.2010-0388

Choi, Y., & Chan, A. P. (2015). PROVEAN web server: a tool to predict the functional effect of amino acid substitutions and indels. *Bioinformatics*, *31*(16), 2745-2747. https://doi.org/10.1093/bioinformatics/btv195

Copeland, D. L., Duff, R. J., Liu, Q., Prokop, J., & Londraville, R. L. (2011). Leptin in teleost fishes: an argument for comparative study. *Frontiers in physiology*, *2*, 26-26. https://doi.org/10.3389/fphys.2011.00026

Daane, J. M., Blum, N., Lanni, J., Boldt, H., Iovine, M. K., Higdon, C. W., Johnson, S. L., Lovejoy, N. R., & Harris, M. P. (2021). Modulation of bioelectric cues in the evolution of flying fishes. *Curr Biol*, *31*(22), 5052-5061 e5058. https://doi.org/10.1016/j.cub.2021.08.054

Daane, J. M., Dornburg, A., Smits, P., MacGuigan, D. J., Brent Hawkins, M., Near, T. J., William Detrich Iii, H., & Harris, M. P. (2019). Historical contingency shapes adaptive radiation in Antarctic fishes. *Nature Ecology & Evolution*, *3*(7), 1102-1109. https://doi.org/10.1038/s41559-019-0914-2

Daane, J. M., Rohner, N., Konstantinidis, P., Djuranovic, S., & Harris, M. P. (2015). Parallelism and Epistasis in Skeletal Evolution Identified through Use of Phylogenomic Mapping Strategies. *Molecular Biology and Evolution*, *33*(1), 162-173. https://doi.org/10.1093/molbev/msv208

Danecek, P., Bonfield, J. K., Liddle, J., Marshall, J., Ohan, V., Pollard, M. O., Whitwham, A., Keane, T., McCarthy, S. A., Davies, R. M., & Li, H. (2021). Twelve years of SAMtools and BCFtools. *GigaScience*, *10*(2), giab008. https://doi.org/10.1093/gigascience/giab008

Davidson, W. S., Koop, B. F., Jones, S. J. M., Iturra, P., Vidal, R., Maass, A., Jonassen, I., Lien, S., & Omholt, S. W. (2010). Sequencing the genome of the Atlantic salmon (Salmo salar). *Genome Biology*, *11*(9), 403. https://doi.org/10.1186/gb-2010-11-9-403

de Graaf, M., Megens, H. J., Samallo, J., & Sibbing, F. (2010). Preliminary insight into the age and origin of the Labeobarbus fish species flock from Lake Tana (Ethiopia) using the mtDNA cytochrome b gene. *Mol Phylogenet Evol*, *54*(2), 336-343. https://doi.org/10.1016/j.ympev.2009.10.029

De-Kayne, R., Selz, O. M., Marques, D. A., Frei, D., Seehausen, O., & Feulner, P. G. D. (2022a). Genomic architecture of adaptive radiation and hybridization in Alpine whitefish. *Nature Communications*, *13*(1), 4479. https://doi.org/10.1038/s41467-022-32181-8

De-Kayne, R., Selz, O. M., Marques, D. A., Frei, D., Seehausen, O., & Feulner, P. G. D. (2022b). Hybridization and a mixture of small and large-effect loci facilitate adaptive radiation. *bioRxiv*, 2022.2002.2018.481029. https://doi.org/10.1101/2022.02.18.481029

Decherf, S., Seugnet, I., Kouidhi, S., Lopez-Juarez, A., Clerget-Froidevaux, M. S., & Demeneix, B. A. (2010). Thyroid hormone exerts negative feedback on hypothalamic type 4 melanocortin receptor expression. *Proc Natl Acad Sci U S A*, *107*(9), 4471-4476. https://doi.org/10.1073/pnas.0905190107

Diaczok, D., Romero, C., Zunich, J., Marshall, I., & Radovick, S. (2008). A Novel Dominant Negative Mutation of OTX2 Associated with Combined Pituitary Hormone Deficiency. *The Journal of Clinical Endocrinology & Metabolism*, *93*(11), 4351-4359. https://doi.org/10.1210/jc.2008-1189

Dimitrieva, S., & Bucher, P. (2013). UCNEbase--a database of ultraconserved non-coding elements and genomic regulatory blocks. *Nucleic acids research*, *41*(Database issue), D101-D109. https://doi.org/10.1093/nar/gks1092

Esin, E. V., Bocharova, E. S., Borisova, E. A., & Markevich, G. N. (2020). Interaction among morphological, trophic and genetic groups in the rapidly radiating Salvelinus fishes from Lake Kronotskoe. *Evolutionary Ecology*, *34*(4), 611-632. https://doi.org/10.1007/s10682-020-10048-y

Esin, E. V., Markevich, G. N., Melnik, N. O., Kapitanova, D. V., & Shkil, F. N. (2021). Natural toxic impact and thyroid signalling interplay orchestrates riverine adaptive divergence of salmonid fish. *J Anim Ecol*, *90*(4), 1004-1019. https://doi.org/10.1111/1365-2656.13429

Esin, E. V., Markevich, G. N., Melnik, N. O., Zlenko, D. V., & Shkil, F. N. (2021). Ambient temperature as a factor contributing to the developmental divergence in sympatric salmonids. *PLOS ONE*, *16*(10), e0258536. https://doi.org/10.1371/journal.pone.0258536

Esin, E. V., Markevich, G. N., & Pichugin, M. Y. (2018). Juvenile divergence in adaptive traits among seven sympatric fish ecomorphs arises before moving to different lacustrine

habitats. *Journal of Evolutionary Biology*, *31*(7), 1018-1034. https://doi.org/https://doi.org/10.1111/jeb.13283

Esin, E. V., Markevich, G. N., Zlenko, D. V., & Shkil, F. N. (2021). Thyroid-Mediated Metabolic Differences Underlie Ecological Specialization of Extremophile Salmonids in the Arctic Lake El'gygytgyn. *Frontiers in Ecology and Evolution*, *9*. https://doi.org/10.3389/fevo.2021.715110

Evans, A. L., & Gage, P. J. (2005). Expression of the homeobox gene Pitx2 in neural crest is required for optic stalk and ocular anterior segment development. *Human Molecular Genetics*, *14*(22), 3347-3359. https://doi.org/10.1093/hmg/ddi365

Fabik, J., Kovacova, K., Kozmik, Z., & Machon, O. (2020). Neural crest cells require Meis2 for patterning the mandibular arch via the Sonic hedgehog pathway. *Biology Open*, *9*(6). https://doi.org/10.1242/bio.052043

Friedrichs, B., Tepel, C., Reinheckel, T., Deussing, J., von Figura, K., Herzog, V., Peters, C., Saftig, P., & Brix, K. (2003). Thyroid functions of mouse cathepsins B, K, and L. *The Journal of Clinical Investigation*, *111*(11), 1733-1745. https://doi.org/10.1172/JCI15990

Hartl, D. L., Clark, A. G., & Clark, A. G. (1997). *Principles of population genetics* (Vol. 116). Sinauer associates Sunderland, MA.

Herrero, J., Muffato, M., Beal, K., Fitzgerald, S., Gordon, L., Pignatelli, M., Vilella, A. J., Searle, S. M. J., Amode, R., Brent, S., Spooner, W., Kulesha, E., Yates, A., & Flicek, P. (2016). Ensembl comparative genomics resources. *Database : the journal of biological databases and curation*, *2016*, bav096. https://doi.org/10.1093/database/bav096

Hoang, D. T., Chernomor, O., von Haeseler, A., Minh, B. Q., & Vinh, L. S. (2017). UFBoot2: Improving the Ultrafast Bootstrap Approximation. *Molecular Biology and Evolution*, *35*(2), 518-522. https://doi.org/10.1093/molbev/msx281

Jacobs, A., Carruthers, M., Yurchenko, A., Gordeeva, N. V., Alekseyev, S. S., Hooker, O., Leong, J. S., Minkley, D. R., Rondeau, E. B., Koop, B. F., Adams, C. E., & Elmer, K. R. (2020). Parallelism in eco-morphology and gene expression despite variable evolutionary and genomic backgrounds in a Holarctic fish. *PLoS Genet*, *16*(4), e1008658. https://doi.org/10.1371/journal.pgen.1008658

Jonsson, B., & Jonsson, N. (2001). Polymorphism and speciation in Arctic charr. *Journal of Fish Biology*, *58*(3), 605-638. https://doi.org/https://doi.org/10.1111/j.1095-8649.2001.tb00518.x

Kalyaanamoorthy, S., Minh, B. Q., Wong, T. K. F., von Haeseler, A., & Jermiin, L. S. (2017). ModelFinder: fast model selection for accurate phylogenetic estimates. *Nature Methods*, *14*(6), 587-589. https://doi.org/10.1038/nmeth.4285

Kitano, J., Lema, S. C., Luckenbach, J. A., Mori, S., Kawagishi, Y., Kusakabe, M., Swanson, P., & Peichel, C. L. (2010). Adaptive divergence in the thyroid hormone signaling pathway in the stickleback radiation. *Current biology : CB*, *20*(23), 2124-2130. https://doi.org/10.1016/j.cub.2010.10.050

Klemetsen, A. (2010). The Charr Problem Revisited: Exceptional Phenotypic Plasticity Promotes Ecological Speciation in Postglacial Lakes. *Freshwater Reviews*, *3*(1), 49-74. https://doi.org/10.1608/frj-3.1.3

Kofler, R., Orozco-terWengel, P., De Maio, N., Pandey, R. V., Nolte, V., Futschik, A., Kosiol, C., & Schlötterer, C. (2011). PoPoolation: A Toolbox for Population Genetic Analysis of Next

Generation Sequencing Data from Pooled Individuals. *PLOS ONE*, *6*(1), e15925. https://doi.org/10.1371/journal.pone.0015925

Kofler, R., Pandey, R. V., & Schlötterer, C. (2011). PoPoolation2: identifying differentiation between populations using sequencing of pooled DNA samples (Pool-Seq). *Bioinformatics (Oxford, England)*, *27*(24), 3435-3436. https://doi.org/10.1093/bioinformatics/btr589

Kozomara, A., & Griffiths-Jones, S. (2010). miRBase: integrating microRNA annotation and deep-sequencing data. *Nucleic acids research*, *39*(suppl_1), D152-D157. https://doi.org/10.1093/nar/gkq1027

Lecaudey, L. A., Schliewen, U. K., Osinov, A. G., Taylor, E. B., Bernatchez, L., & Weiss, S. J. (2018). Inferring phylogenetic structure, hybridization and divergence times within Salmoninae (Teleostei: Salmonidae) using RAD-sequencing. *Molecular Phylogenetics and Evolution*, *124*, 82-99. https://doi.org/https://doi.org/10.1016/j.ympev.2018.02.022

Levin, B. A., Simonov, E., Dgebuadze, Y. Y., Levina, M., & Golubtsov, A. S. (2020). In the rivers: Multiple adaptive radiations of cyprinid fishes (Labeobarbus) in Ethiopian Highlands. *Scientific Reports*, *10*(1), 7192. https://doi.org/10.1038/s41598-020-64350-4

Li, H., Handsaker, B., Wysoker, A., Fennell, T., Ruan, J., Homer, N., Marth, G., Abecasis, G., Durbin, R., & Subgroup, G. P. D. P. (2009). The Sequence Alignment/Map format and SAMtools. *Bioinformatics*, *25*(16), 2078-2079. https://doi.org/10.1093/bioinformatics/btp352

Liu, X., Wang, H., Li, G., Huang, H.-Z., & Wang, Y.-Q. (2013). The function of *DrPax1b* gene in the embryonic development of zebrafish. *Genes & Genetic Systems*, *88*(4), 261-269. https://doi.org/10.1266/ggs.88.261

Liu, Y.-H., Lin, T.-C., & Hwang, S.-P. L. (2020). Zebrafish Pax1a and Pax1b are required for pharyngeal pouch morphogenesis and ceratobranchial cartilage development. *Mechanisms of Development*, *161*, 103598. https://doi.org/https://doi.org/10.1016/j.mod.2020.103598

Ma, Z., Zhu, P., Pang, M., Guo, L., Chang, N., Zheng, J., Zhu, X., Gao, C., Huang, H., Cui, Z., Xiong, J. W., Peng, J., & Chen, J. (2017). A novel inducible mutagenesis screen enables to isolate and clone both embryonic and adult zebrafish mutants. *Sci Rep*, *7*(1), 10381. https://doi.org/10.1038/s41598-017-10968-w

Maitland, P. S., Winfield, I. J., McCarthy, I. D., & Igoe, F. (2007). The status of Arctic charr Salvelinus alpinus in Britain and Ireland. *Ecology of Freshwater Fish*, *16*(1), 6-19. https://doi.org/https://doi.org/10.1111/j.1600-0633.2006.00167.x

Malinsky, M., Challis, R. J., Tyers, A. M., Schiffels, S., Terai, Y., Ngatunga, B. P., Miska, E. A., Durbin, R., Genner, M. J., & Turner, G. F. (2015). Genomic islands of speciation separate cichlid ecomorphs in an East African crater lake. *Science*, *350*(6267), 1493-1498. https://doi.org/10.1126/science.aac9927

Malinsky, M., Matschiner, M., & Svardal, H. (2021). Dsuite - Fast D-statistics and related admixture evidence from VCF files. *Mol Ecol Resour*, *21*(2), 584-595. https://doi.org/10.1111/1755-0998.13265

Malinsky, M., Svardal, H., Tyers, A. M., Miska, E. A., Genner, M. J., Turner, G. F., & Durbin, R. (2018). Whole-genome sequences of Malawi cichlids reveal multiple radiations

interconnected by gene flow. *Nat Ecol Evol*, *2*(12), 1940-1955. https://doi.org/10.1038/s41559-018-0717-x

Markevich, G., Esin, E., & Anisimova, L. (2018). Basic description and some notes on the evolution of seven sympatric morphs of Dolly Varden Salvelinus malma from the Lake Kronotskoe Basin. *Ecol Evol*, *8*(5), 2554-2567. https://doi.org/10.1002/ece3.3806

Markevich, G. N., Zlenko, D. V., Shkil, F. N., Schliewen, U. K., Anisimova, L. A., Sharapkova, A. A., & Esin, E. V. (2021). Natural Barriers and Internal Sources for the Reproductive Isolation in Sympatric Salmonids from the Lake–River System. *Evolutionary Biology*, *48*(4), 407-421. https://doi.org/10.1007/s11692-021-09546-w

Mason, V. C., Li, G., Helgen, K. M., & Murphy, W. J. (2011). Efficient cross-species capture hybridization and next-generation sequencing of mitochondrial genomes from noninvasively sampled museum specimens. *Genome research*, *21*(10), 1695-1704. https://doi.org/10.1101/gr.120196.111

McCormick, S. D. (2012). 5 - Smolt Physiology and Endocrinology. In S. D. McCormick, A. P. Farrell, & C. J. Brauner (Eds.), *Fish Physiology* (Vol. 32, pp. 199-251). Academic Press. https://doi.org/https://doi.org/10.1016/B978-0-12-396951-4.00005-0

McCormick, S. D., Regish, A. M., Ardren, W. R., Bjornsson, B. T., & Bernier, N. J. (2019). The evolutionary consequences for seawater performance and its hormonal control when anadromous Atlantic salmon become landlocked. *Sci Rep*, *9*(1), 968. https://doi.org/10.1038/s41598-018-37608-1

McCormick, S. D., Regish, A. M., Ardren, W. R., Björnsson, B. T., & Bernier, N. J. (2019). The evolutionary consequences for seawater performance and its hormonal control when anadromous Atlantic salmon become landlocked. *Scientific Reports*, *9*(1), 968. https://doi.org/10.1038/s41598-018-37608-1

McLean, C. Y., Bristor, D., Hiller, M., Clarke, S. L., Schaar, B. T., Lowe, C. B., Wenger, A. M., & Bejerano, G. (2010). GREAT improves functional interpretation of cis-regulatory regions. *Nature biotechnology*, *28*(5), 495-501. https://doi.org/10.1038/nbt.1630

Myers, G. S. (1960). The Endemic Fish Fauna of Lake Lanao, and the Evolution of Higher Taxonomic Categories. *Evolution*, *14*(3), 323-333. https://doi.org/10.2307/2405975

Nagelkerke, L., & Sibbing, F. A. (2000). The large barbs (Barbus SPP., cyprinidae, teleostei) of Lake Tana (Ethiopia), with a description of a new species, Barbus osseensis. *Netherlands Journal of Zoology 50 (2000) 2*, *50*. https://doi.org/10.1163/156854200505946

Nagelkerke, L. A., Leon-Kloosterziel, K. M., Megens, H. J., De Graaf, M., Diekmann, O. E., & Sibbing, F. A. (2015). Shallow genetic divergence and species delineations in the endemic Labeobarbus species flock of Lake Tana, Ethiopia. *J Fish Biol*, *87*(5), 1191-1208. https://doi.org/10.1111/jfb.12779

Ng, P. C., & Henikoff, S. (2003). SIFT: Predicting amino acid changes that affect protein function. *Nucleic acids research*, *31*(13), 3812-3814. https://doi.org/10.1093/nar/gkg509

Nguyen, L.-T., Schmidt, H. A., von Haeseler, A., & Minh, B. Q. (2015). IQ-TREE: A Fast and Effective Stochastic Algorithm for Estimating Maximum-Likelihood Phylogenies. *Molecular Biology and Evolution*, *32*(1), 268-274. https://doi.org/10.1093/molbev/msu300

Nordeng, H. (1983). Solution to the "Char Problem" based on Arctic Char (Salvelinus alpinus) in Norway. *Canadian Journal of Fisheries and Aquatic Sciences*, *40*(9), 1372-1387. https://doi.org/10.1139/f83-159

Osinov, A. G., Volkov, A. A., & Mugue, N. S. (2021). Charrs of the genus Salvelinus (Salmonidae): hybridization, phylogeny and evolution. *Hydrobiologia*, *848*(3), 705-726. https://doi.org/10.1007/s10750-020-04478-6

Purcell, S., Neale, B., Todd-Brown, K., Thomas, L., Ferreira, M. A., Bender, D., Maller, J., Sklar, P., de Bakker, P. I., Daly, M. J., & Sham, P. C. (2007). PLINK: a tool set for whole-genome association and population-based linkage analyses. *American journal of human genetics*, *81*(3), 559-575. https://doi.org/10.1086/519795

Quinlan, A. R., & Hall, I. M. (2010). BEDTools: a flexible suite of utilities for comparing genomic features. *Bioinformatics*, *26*(6), 841-842. https://doi.org/10.1093/bioinformatics/btq033

Quinlan, A. R., & Hall, I. M. (2010). BEDTools: a flexible suite of utilities for comparing genomic features. *Bioinformatics*, *26*(6), 841-842. https://doi.org/10.1093/bioinformatics/btq033

Richard, S., Guyot, R., Rey-Millet, M., Prieux, M., Markossian, S., Aubert, D., & Flamant, F. (2020). A Pivotal Genetic Program Controlled by Thyroid Hormone during the Maturation of GABAergic Neurons. *iScience*, *23*(3), 100899-100899. https://doi.org/10.1016/j.isci.2020.100899

Rondeau, E. B., Minkley, D. R., Leong, J. S., Messmer, A. M., Jantzen, J. R., von Schalburg, K. R., Lemon, C., Bird, N. H., & Koop, B. F. (2014). The Genome and Linkage Map of the Northern Pike (Esox lucius): Conserved Synteny Revealed between the Salmonid Sister Group and the Neoteleostei. *PLOS ONE*, *9*(7), e102089. https://doi.org/10.1371/journal.pone.0102089

Rothstein, M., & Simoes-Costa, M. (2020). Heterodimerization of TFAP2 pioneer factors drives epigenomic remodeling during neural crest specification. *Genome research*, *30*(1), 35-48. https://doi.org/10.1101/gr.249680.119

Sandlund, O. T., Gunnarsson, K., Jónasson, P. M., Jonsson, B., Lindem, T., Magnússon, K. P., Malmquist, H. J., Sigurjónsdóttir, H., Skúlason, S., & Snorrason, S. S. (1992). The Arctic Charr Salvelinus alpinus in Thingvallavatn. *Oikos*, *64*(1/2), 305-351. https://doi.org/10.2307/3545056

Sedlazeck, F. J., Rescheneder, P., & von Haeseler, A. (2013). NextGenMap: fast and accurate read mapping in highly polymorphic genomes. *Bioinformatics*, *29*(21), 2790-2791. https://doi.org/10.1093/bioinformatics/btt468

Shkil, F. N., Kapitanova, D. V., Borisov, V. B., Abdissa, B., & Smirnov, S. V. (2012). Thyroid hormone in skeletal development of cyprinids: effects and morphological consequences. *Journal of Applied Ichthyology*, *28*(3), 398-405. https://doi.org/https://doi.org/10.1111/j.1439-0426.2012.01992.x

Shkil, F. N., Lazebnyi, O. E., Kapitanova, D. V., Abdissa, B., Borisov, V. B., & Smirnov, S. V. (2015). Ontogenetic mechanisms of explosive morphological divergence in the Lake Tana (Ethiopia) species flock of large African barbs (Labeobarbus; Cyprinidae; Teleostei). *Russian Journal of Developmental Biology*, *46*(5), 294-306. https://doi.org/10.1134/S1062360415050069

Simonsen, M. K., Siwertsson, A., Adams, C. E., Amundsen, P.-A., Præbel, K., & Knudsen, R. (2017). Allometric trajectories of body and head morphology in three sympatric Arctic

charr (Salvelinus alpinus (L.)) morphs. *Ecology and Evolution*, *7*(18), 7277-7289. https://doi.org/https://doi.org/10.1002/ece3.3224

Taylor, E. B. (2016). The Arctic char (Salvelinus alpinus) “complex” in North America revisited. *Hydrobiologia*, *783*(1), 283-293. https://doi.org/10.1007/s10750-015-2613-6

Tingaud-Sequeira, A., Trimouille, A., Marlin, S., Lopez, E., Berenguer, M., Gherbi, S., Arveiler, B., Lacombe, D., & Rooryck, C. (2020). Functional and genetic analyses of ZYG11B provide evidences for its involvement in OAVS. *Molecular Genetics & Genomic Medicine*, *8*(10), e1375. https://doi.org/https://doi.org/10.1002/mgg3.1375

Tipsmark, C. K., Sørensen, K. J., & Madsen, S. S. (2010). Aquaporin expression dynamics in osmoregulatory tissues of Atlantic salmon during smoltification and seawater acclimation. *Journal of Experimental Biology*, *213*(3), 368-379. https://doi.org/10.1242/jeb.034785

Treaster, S., Deelen, J., Daane, J. M., Murabito, J., Karasik, D., & Harris, M. P. (2022). *Nature Portfolio*. https://doi.org/10.21203/rs.3.rs-1126287/v1

Viktorovskii, R. M. (1978). *Mekhanizm vidoobrazovaniya u gol'tsov Kronotskogo Ozera*. Изд-во Наука.

Walker, A. F., Greer, R. B., & Gardner, A. S. (1988). Two ecologically distinct forms of arctic charr Salvelinus alpinus (L.) in Loch Rannoch, Scotland. *Biological Conservation*, *43*(1), 43-61. https://doi.org/https://doi.org/10.1016/0006-3207(88)90077-8

Wong, T. C. B., Rebbert, M., Wang, C., Chen, X., Heffer, A., Zarelli, V. E., Dawid, I. B., & Zhao, H. (2016). Genes regulated by potassium channel tetramerization domain containing 15 (Kctd15) in the developing neural crest. *The International journal of developmental biology*, *60*(4-6), 159-166. https://doi.org/10.1387/ijdb.160058id

Yagasaki, Y., Yamaguchi, T., Watahiki, J., Konishi, M., Katoh, H., & Maki, K. (2003). The role of craniofacial growth in leptin deficient (ob/ob) mice [https://doi.org/10.1034/j.1600-0544.2003.00260.x]. *Orthodontics & Craniofacial Research*, *6*(4), 233-241. https://doi.org/https://doi.org/10.1034/j.1600-0544.2003.00260.x

Yoon, G. H., Kim, K., Park, D. S., & Choi, S. C. (2022). RNF152 negatively regulates Wnt/β-catenin signaling in Xenopus embryos. *BMB Rep*.

Zimmermann-Belsing, T., Brabant, G., Holst, J., & Feldt-Rasmussen, U. (2003). Circulating leptin and thyroid dysfunction. *European Journal of Endocrinology Eur J Endocrinol*, *149*(4), 257-271. https://doi.org/10.1530/eje.0.1490257